USING ENERGY STORAGE SYSTEM TO IMPROVE POWER SYSTEM INERTIA

(VIRTUAL INERTIA)

J.M. Gallage

(170172R)

M.B.B.N. Medawatta

(170384T)

M.D.D. Perera

(170439T)

Degree of Bachelor of Science of Engineering

Department of Electrical Engineering

University of Moratuwa

Sri Lanka

July 2022

USING ENERGY STORAGE SYSTEM TO IMPROVE POWER SYSTEM INERTIA

(VIRTUAL INERTIA)

J.M. Gallage

(170172R)

M.B.B.N. Medawatta

(170384T)

M.D.D. Perera

(170439T)

Report submitted in partial fulfillment of the requirements for the degree Bachelor of Science of Engineering in Electrical Engineering

Department of Electrical Engineering

University of Moratuwa

Sri Lanka

July 2022

Declaration, copyright statement and the statement of the supervisor

We declare that this is our own work and this report does not incorporate without acknowledgement any material previously submitted for a Degree or Diploma in any other University or institute of higher learning and to the best of our knowledge and belief it does not contain any material previously published or written by another person except where the acknowledgement is made in the text.

Also, we hereby grant to University of Moratuwa the non-exclusive right to reproduce and distribute our report, in whole or in part in print, electronic or other medium. We retain the right to use this content in whole or part in future works (such as articles or books).

Signature (J.M.Gallage):  Date: 25/07/2022

Signature (M.B.B.N. Medawatta): 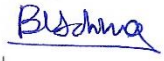 Date: 25/07/2022

Signature (M.D.D. Perera):  Date: 25/07/2022

The above candidates have carried out research for the B.Sc. report under my supervision.

Name of the supervisor: Dr. Asanka Rodrigo

Signature of the supervisor: 

Date: 25/07/2022

Abstract

The main focus of this paper is to address the instability that occur in the modern power system due to integration of Renewable energy sources (RESs) with power electronic converters. The integration of renewables like wind and solar results in reduced grid inertia stability due to their lack of inertia.

In order to increase the RESs share in the energy mix further, the lack of inertia must be compensated with alternative method to reduce the instability of the system due to reduction of grid inertia. To improve the inertia in the system energy storage system can be used as a virtual synchronous generator (VSG) or virtual inertia systems to emulate inertia to increase the frequency stability of a power system

In this report a virtual inertia system and its operation is described. The validity of the described system is evaluated using MATLAB/Simulink simulations.

Dedication

This report is dedicated to our families and many friends who continuously encouraged and supported us with our academic work. We will always appreciate all they have done for us, especially our parents who gave us the required financial and moral support to complete this design work.

Acknowledgement

This design project would not have been possible without the support of many people. Special thanks to our supervisor, Dr. W.D.A.S. Rodrigo, who mentored our team and supported continuously, advised and directed and helped to make some sense of the confusions we went through.

Also, thanks to our progress review panel members Prof. S. Kumarawadu, Prof. J.P. Karunadasa and Dr. L.N. Widanagama Arachchige who offered guidance, feedback and support.

Finally, thanks to the Department of Electrical Engineering of University of Moratuwa for this opportunity and thanks to numerous friends who helped us in this long process offering support.

Table of contents

List of Figures

List of Tables

List of abbreviations

BESS – Battery Energy Storage Systems

RES – Renewable Energy Sources

PLL – Phase Locked Loop

RoCoF – Rate of Change of Frequency

VSG – Virtual Synchronous Generator

1. Introduction

Due to environmental concerns and rapid development of the technology integration of RESs to the power system is accelerating fast and replacing the traditional fossil fuel based conventional power plant with power electronics based RESs like wind and solar which lack inertia [1]. Kinetic energy that stored in rotating synchronous generator provide inertia to the power system which helps to stabilize the frequency of the system. When the system inertia is too low the ability to withstand a disturbance to the system get reduced so once the frequency of the system gets out of the predefined safety region the entire power system could collapse [2].

In order to reduce the effect of low inertia in the power system, it is proposed to use virtual inertia systems with energy storage systems. With a suitable controller technique, the VSG has the ability to mimic the dynamic characteristics of the synchronous generator [3]. Compared with the synchronous generator VSG has more advantages like ability to change characteristics by changing parameters in real-time, operation flexibility etc.

Most literatures available about VSG control techniques uses mainly two approaches. First is to solve the swing equation numerically to calculate the load angle and then inject the power by varying the load angle. The approach used here is to use the rate of change of frequency (RoCoF) to calculate the required real power that needs to be injected to aid frequency stability. In this method, numerically solving the swing equation is avoided and the calculated power is injected by directly changing the phase angle between the inverter output and the grid voltages.

2. Literature Review

Due to environmental concerns, the importance of renewable energy has increased over the years. Due to the intermittent nature of renewables, the power grid should be a mixture of converter based renewable power plant and synchronous generator based conventional power plants.

However, the integration of renewables could have a negative effect on the stability of a power system due to their lack of usable inertia. In order to improve power system inertia under renewable integration, various virtual inertia methods have been proposed.

The main methods discussed uses a separate energy storage to emulate the kinetic energy stored in the rotor of a synchronous generator. A suitable control system is required to supply power to the grid in a similar manner to how a synchronous generator expends its kinetic energy. Even amongst energy storage methods, there are different approaches used.

Some important highlights from literature are discussed here. From research paper, "Power System Stabilization Using Virtual Synchronous Generator with Alternating Moment of Inertia" by J. Alipoor, Y. Miura and T. Ise. [1]

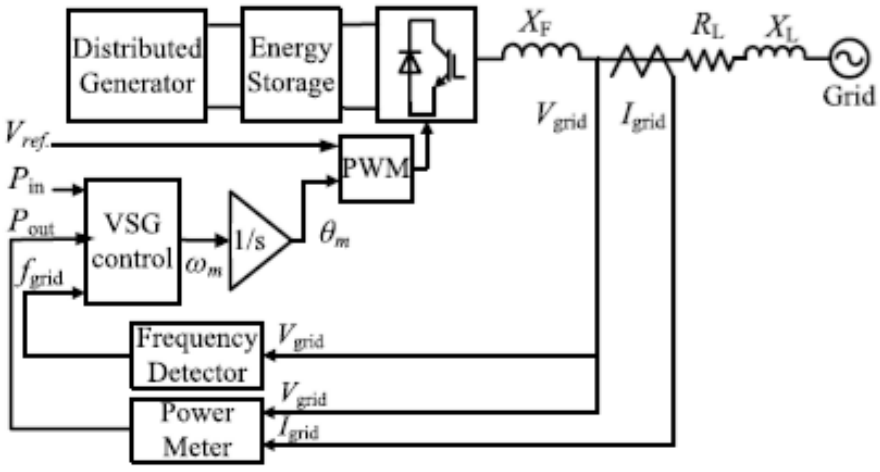

Figure 2.1: Block diagram of VSG unit

Source: Power System Stabilization Using Virtual Synchronous Generator with Alternating Moment of Inertia" by J. Alipoor, Y. Miura and T. Ise.

This model numerically solves the swing equation to calculate the virtual rotor speed and integrates it to obtain the load angle Virtual inertia constant alternates between 2 set values depending on the sign of frequency deviation and rate of change of frequency this allows for faster stabilization. The power output of this model cannot make step changes in power output. This can result in slower response. The concept of alternating inertia was implemented into our own design.

From research paper "Self-Tuning Virtual Synchronous Machine: A Control Strategy for Energy Storage Systems to Support Dynamic Frequency Control" by, M. A. Torres L., L. A. C. Lopes, L. A. Morán T., and J. R. Espinoza C. [2]

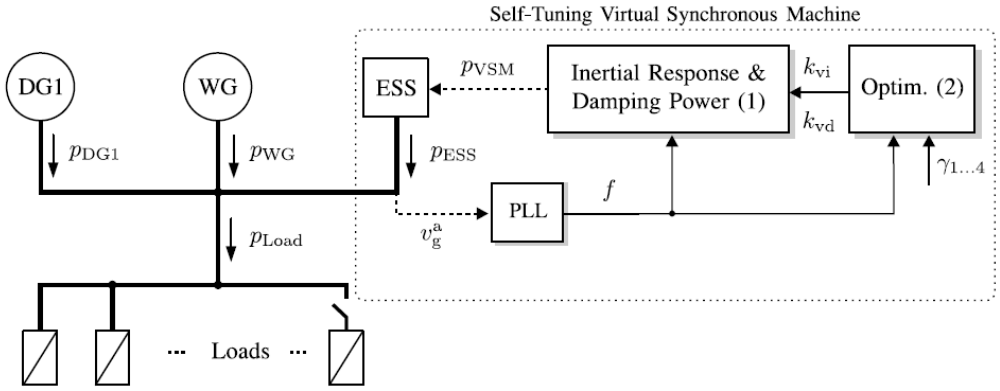

Figure 2.2: ST-VSM with variable inertia and damping

Source: Self-Tuning Virtual Synchronous Machine: A Control Strategy for Energy Storage Systems to Support Dynamic Frequency Control" by, M. A. Torres L., L. A. C. Lopes, L. A. Morán T., and J. R. Espinoza C.

In this paper, a sperate energy source is controlled directly to supply/absorb power from the grid under disturbances and does not necessarily provide power to the grid at steady state, in this method, a virtual rotor angle is not simulated. And no numerical solving of swing equations is present.

This system controls injected power directly from the rate of change of frequency and therefore, step changes of power are theoretically possible. This system also has a parameter optimization process to find the most suitable parameters for the

operation of the virtual inertia system. This is what is defined as a “self-tuning” virtual inertia system. This provides an improved response due to parameter optimization. However, the parameter optimization introduces significant mathematical and computational complexity.

From the paper, "Enhanced Virtual Synchronous Generator Control for Parallel Inverters in Microgrids” by J. Liu, Y. Miura, H. Bevrani and T. Ise. [3]

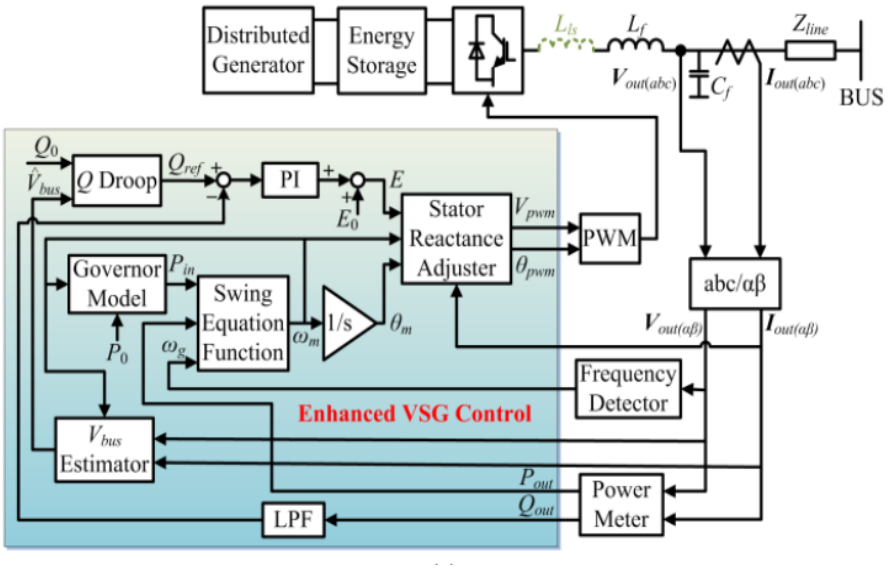

Figure 2.3: Block diagram of the proposed enhanced VSG control

Source: Enhanced Virtual Synchronous Generator Control for Parallel Inverters in Microgrids” by J. Liu, Y. Miura, H. Bevrani and T. Ise.

This model is also similar in operation to the model discussed in [1] with the addition of a reactive power control and the inertial action is mostly similar.

From the paper, “Grid Tied Converter with Virtual Kinetic Storage” by M.P.N van Wesenbeeck, S.W.H. de Haan, P. Varela, K. Visscher. [4]. The system described in this paper measures the rate of change of frequency and the frequency deviation to inject power into the grid during disturbances. This system also does not perform numerical solving of swing equation.

It is worth noting that most virtual inertia systems fall under two categories. They are,

1. Systems that numerically solve the swing equation to calculate the load angle
2. Systems that directly calculate the power to be injected using the rate of change of frequency and frequency deviation.

Controlling the power supplied to the microgrid by adjusting the load angle is an important idea for this project. Modern inverters can control their phase angle relative to a reference signal using a phase locked loop system (PLL)

This is discussed in detail in “Phase Locked Loop Control of Inverters in a Microgrid” by Matthew Surprenant, Ian Hiskens, Giri Venkataramanan. [5] In this paper, a reference power is supplied to the grid by controlling the phase angle difference between the grid and the inverter. A PLL system tracks the grid side voltage and the inverter maintains the phase angle difference to control the power to the grid.

3. Principle of operation

3.1 Inertia of a synchronous generator

When the equilibrium between the mechanical power input and the electrical power output of a synchronous generator is disrupted by a sudden load change, two aspects of a generator have to be controlled, voltage and power output. Since the time constants of the voltage control systems are extremely small, the voltage is maintained without any noticeable changes. However, the larger time constants associated with the generator prime mover places constraints on the rate of change of mechanical power.

Therefore, the change in mechanical power has a noticeable delay. This power imbalance causes the rotor to expend its kinetic energy and reduce its speed and therefore the output frequency.

The above phenomena can be represented by the following equations.

$$E_k = \frac{1}{2} J\omega^2$$

$$J\omega \frac{d\omega}{dt} = P_m - P_e$$

Here, the symbols have the following definitions.

E_k – Kinetic energy of the rotor

J – Inertia of rotating assembly

ω – Angular frequency of the rotor

P_m – Mechanical energy input

P_e – Electrical energy output

3.2 The concept of virtual inertia

Unlike synchronous generators, converter-based sources such as solar and wind does not consist of inherently deployable short-term energy storages. Therefore, integration of these systems results in a decrease of system inertia. However, this effect can be countered by using short term energy storages such as battery energy storage systems (BESS), supercapacitors etc. to represent the kinetic energy stored in the rotor of a synchronous generator and a suitable control strategy can be employed to inject power into the grid and reduce the kinetic energy expended by the rotors. This results in reduced frequency fluctuations due to the oscillations of the rotors.

Similar to the swing equation of the generators, an equation for the rate of change of rotor kinetic energy can be observed.

$$\Delta P = k\frac{df}{dt}$$

$$k = 2\pi J\omega$$

Here, the fractional change of rotor angular velocity is negligible, therefore the product of moment of inertia and angular velocity can be approximated to a constant. by representing the power values in electrical quantities, we obtain the following equation.

$$\frac{EV\ sin\,\delta}{X} = \frac{EV\ sin\,\delta_0}{X} + k\frac{df}{dt}$$

By rearranging the above equation and incorporating damping,

$$\delta = sin^{-1}(sin\delta_0 + K\frac{df}{dt} + D(f - f^*))$$

$$K = \frac{kX}{EV}$$

The symbols have the following definitions

E – Inverter terminal voltage/ voltage of the virtual inertia system

V – Grid voltage at the point of connection

X – Reactance between the grid and the inverter

δ – Phase angle between the grid and inverter voltages

δ_0 – Initial phase angle between the grid and inverter voltages (Steady state)

f – System frequency

f^* – frequency the system will reach in the next steady state

D – Virtual damping constant

When the system is functioning as a dedicated virtual inertia system, the steady state power is set to zero. Hence, δ_0 is set to zero.

3.3 The concept of alternating inertia

The inertia of a system resists both accelerations and decelerations. Therefore, a high inertia system not only resists the initial frequency drop but also resists returning to the steady state value.

The inherent inertia of a system is a constant. Therefore, this effect can be considered as a tradeoff associated with a high inertia system. However, a virtual inertia system can simply vary its parameters to control the inertia system during various regions of oscillations.

The alternating inertia criteria can be defined as follows.

$$\Delta f = f_0 - f$$

f_0 represents the nominal system frequency.

Table 3.1: Dynamic inertia strategy

	$\Delta f > 0$	$\Delta f < 0$
$\frac{df}{dt} > 0$	Low inertia	High inertia
$\frac{df}{dt} < 0$	High inertia	Low inertia

When the frequency is increasing towards the nominal value, a low inertia setting is selected, when the frequency is increasing away from the nominal value, a high inertia value is selected

When the frequency is decreasing away from the nominal value, a high inertia value is selected and when the frequency is decreasing towards the nominal value, a low value is selected.

In the region where a low inertia value is selected, it is possible to actively reduce the inertia of the system by changing the sign of the inertia parameter of the

virtual inertia control. This allows for faster stabilization by providing a lower value when its beneficial.

For $K > 0$ the system provides negative inertia

For $K < 0$ the system provides positive inertia (similar to a normal generator)

However, setting a negative value for both situations allow for easier tuning.

3.4 Control of damping action

In a synchronous generator, damping action is mainly provided by the damper winding and this action happens naturally without any external control. In a virtual inertia system, the damping action needs to be controlled separately.

The damping power is defined by the term,

$$D(f - f^*)$$

Here, f^* is the frequency that the system will reach in its next steady state. Because the damping action should cease to exist under steady state operation, f^* cannot be kept a constant and needs to be supplied as variable to the virtual inertia system. This can be achieved in two methods.

Method I

By measuring the electrical power output of the generator instantly after the disturbance, it is possible to calculate the next steady state frequency by using the droop characteristics of the generator governor system using the droop equation.

$$f^* = \frac{P}{P_{max}}(f_{FL} - f_{NL}) + f_{NL}$$

P - Power output of the generator

P_{max} - Maximum power output of the generator

f_{NL} - Full load frequency

f_{NL} - No load frequency

In this method, the governor characteristics need to be fed to the virtual inertia controller in order to calculate the next steady state frequency. However, this can lead to errors as the governor parameters can change due to numerous external factors.

Method II

This method uses a sample and hold technique defined below.

$$f_L \leq f \leq f_U \Rightarrow f^* = f(Sample)$$

Otherwise, f^* holds its last value that satisfies the above inequality. (Hold)

Here, f_L, f_U are lower and upper frequency bands defined according to the steady state frequency limits of the generator.

Therefore, when the generator reaches its steady state, $f^* - f$ becomes zero and the damping action is reduced to zero. Note that the damping action is only present when the transient frequency goes out of the steady state frequency limits of the generator. Therefore, the effect of damping is somewhat reduced compared to the previously discussed method. Method II was selected to be implemented in the simulation because it requires fewer external measurements and less additional parameters. When considering a practical scenario, the aforementioned advantages still hold their validity.

3.5 Control block diagram

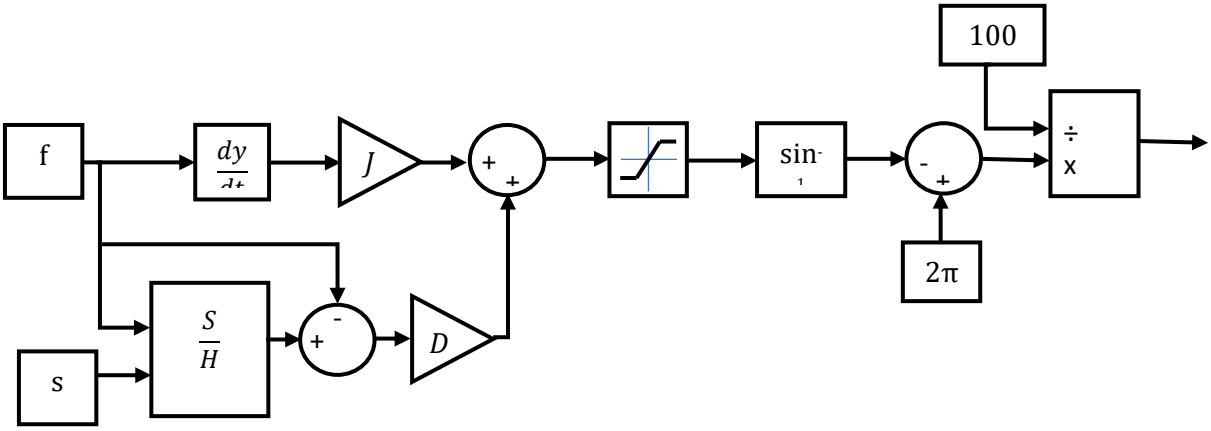

Figure 3.1: Simplified control block diagram

A simplified control block diagram is shown in Figure 3.1 using the constant inertia method. In the alternating inertia method, the logic defined by the Table 3.1 is employed to control the system such that it chooses between the 2 preset inertia values.

In a practical implementation, the inverter is supplied directly with the phase angle or a time delay to the reference signal. The PLL (Phase Locked Loop) system is responsible for controlling the phase angle difference between the grid and inverter/virtual inertia system voltages.

3.6 Stability of the system

The virtual inertia system injects/absorbs power to and from the grid during frequency fluctuations, the operation of the virtual inertia system itself affects the frequency fluctuations of the system. The parameters of the virtual inertia system should be selected such that it does not lead to instability.

The power of the virtual inertia system can be given by,

$$P = K_0 \frac{d\omega}{dt} + D_0(\omega - \omega^*)$$

$$K_0 < 0$$

For a given load step, ω^* is constant therefore this can be modified to obtain the following,

$$\Delta P = K_0 \frac{d\Delta\omega}{dt} + D_0\Delta\omega$$

Applying the Laplace transform gives,

$$\mathcal{L}(\Delta P) = K_0\mathcal{L}\left(\frac{d\Delta\omega}{dt}\right) + D_0\mathcal{L}(\Delta\omega)$$

This gives the transfer function of the virtual inertia system as,

$$\frac{\Delta P(s)}{\Delta\omega(s)} = K_0 s + D_0$$

The following notation is used to denote the Laplace transforms of power and angular speed,

$$\mathcal{L}(\Delta P) = \Delta P(s)$$

$$\mathcal{L}(\Delta\omega) = \Delta\omega(s)$$

We can modify the frequency control block diagram of an isolated power system by adding the transfer function of the virtual inertia system to represent the overall system as shown in Figure 3.2.

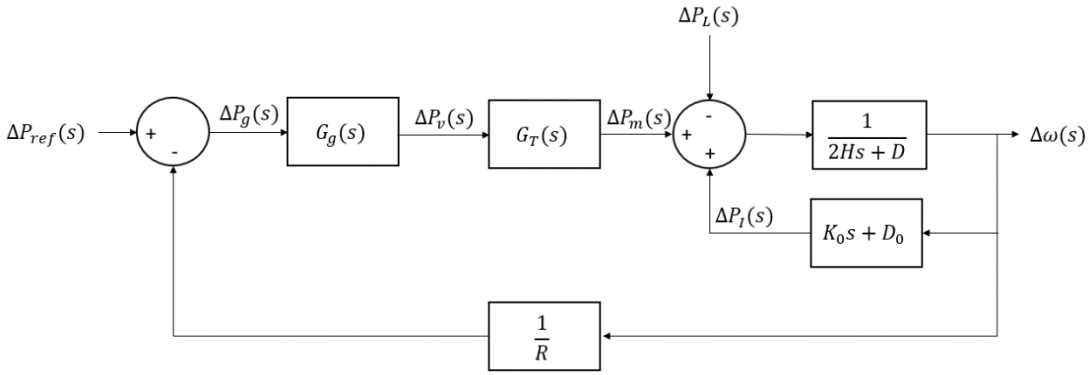

Figure 3.2: Modified frequency control block diagram

Assume a constant reference power,

$$\Delta P_{ref}(s) = 0$$

The virtual inertia system is set to deliver zero power at steady state; therefore, frequency sensitivity is set to zero (at steady state),

$$D_0 = 0$$

Closed loop transfer function of the system is,

$$\frac{\Delta\omega(s)}{\Delta P_L(s)} = \frac{-R}{G_g(s)G_T(s) + R(2Hs - K_0 s - D_0 + D)}$$

Now, the system can be analyzed using standard control system theory. The characteristic equation of the system is,

$$G_g(s)G_T(s) + R(2Hs - K_0 s - D_0 + D) = 0$$

Using the Routh – Hurwitz stability criterion, we can obtain a constraint for parameter controlling the inertial action of the virtual inertia system.

The steady state frequency drop is unaffected by the virtual inertia system. It is given by,

$$\Delta\omega_{ss} = \frac{-\Delta P_L R}{G_g(0)G_T(0) + RD}$$

The symbols have the following definitions

$G_g(s)$ – Transfer function of the governor

$G_T(s)$ – Transfer function of the prime mover/turbine

$\Delta\omega$ – Change in angular velocity

ΔP – Change of power of the virtual inertia system

H – Inertia constant of the synchronous generator

D – Frequency sensitivity of the load

K_0 – Virtual inertia parameter

D_0 – Virtual damping parameter

ΔP_L – Load step

$\Delta\omega_{ss}$ – Steady state frequency drop

4. MATLAB Simulink design and results

4.1 MATLAB Simulink design

In order to simulate and test this model, we use MATLAB modelling. To simulate a system with constant virtual inertia J, system in Figure 4.1 is designed.

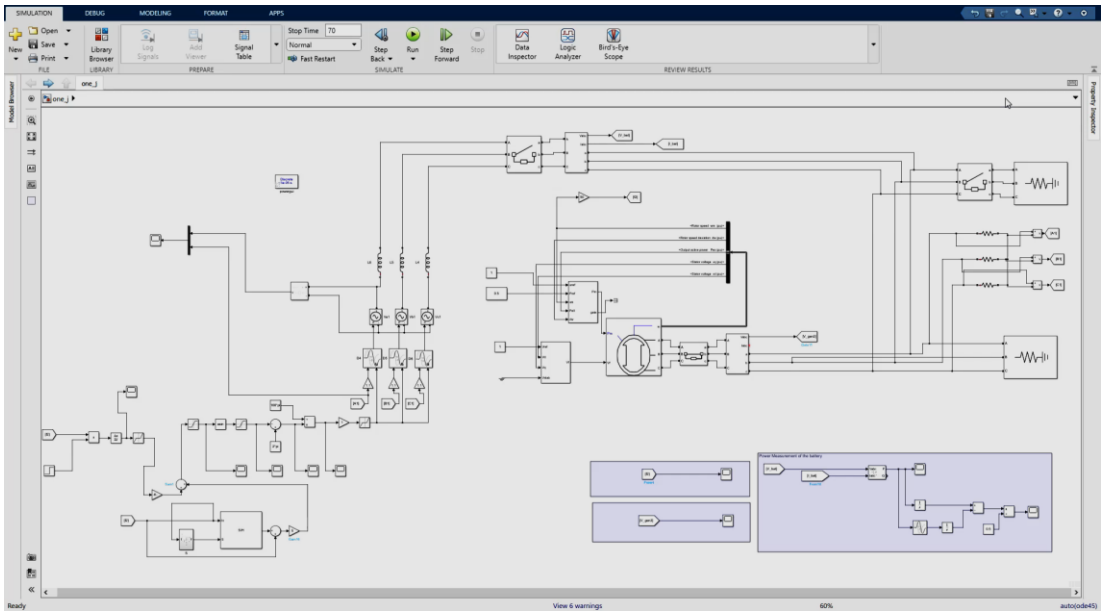

Figure 4.1: MATLAB model for constant virtual inertia system

To simulate the effect of alternating virtual inertia J, system in Figure 4.2 is designed

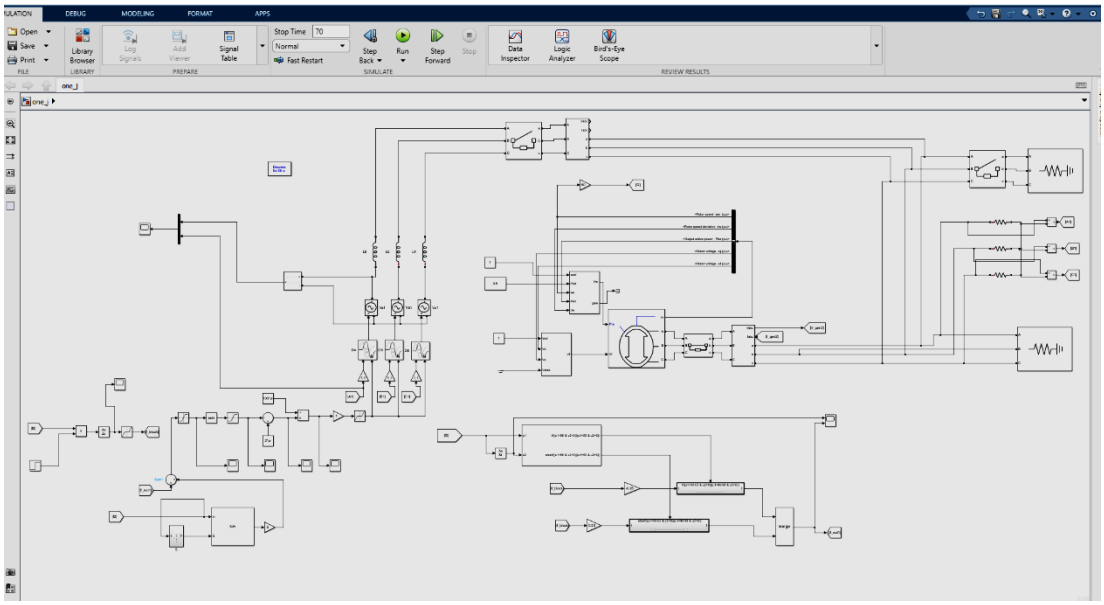

Figure 4.2: MATLAB model for alternating virtual inertia system

In order to simulate the conditions in a multi generator system, system in Figure 4.3 with 3 generators is designed.

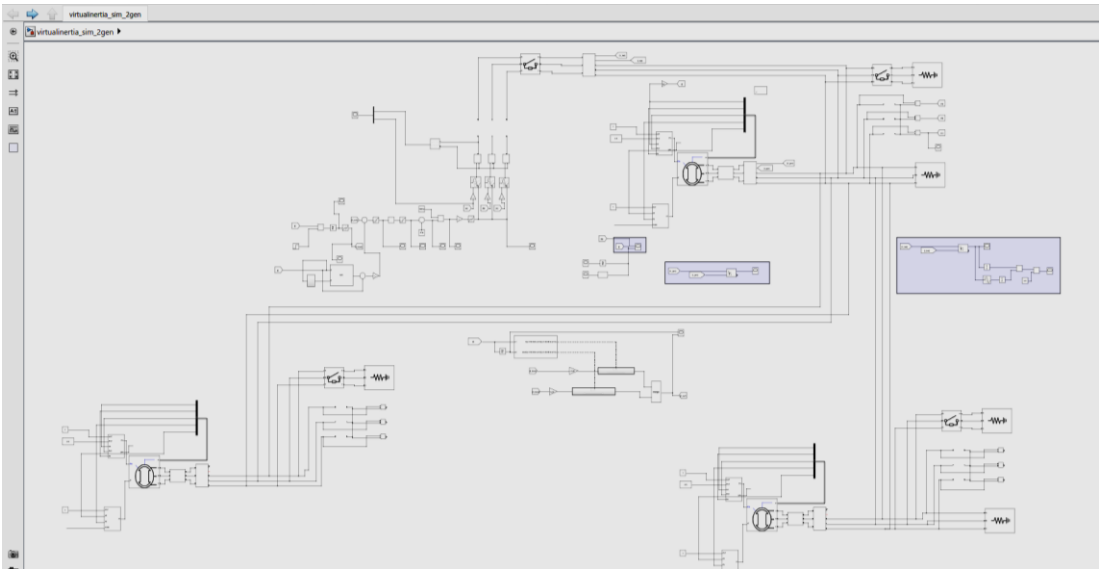

Figure 4.3: MATLAB model for multi generator system

4.2 Results and test conditions for the microgrid system

Specifications for the microgrid system,

Nominal load = 50kW

System voltage = 400V

Inverter/voltage source voltage = 450V

Nominal frequency = 50Hz

J = -0.06s^2

D = 0.1s

Generator inertia = 8.105kgm^2

(i) Results of the system for 5% disturbance from the nominal load (2.5kW)

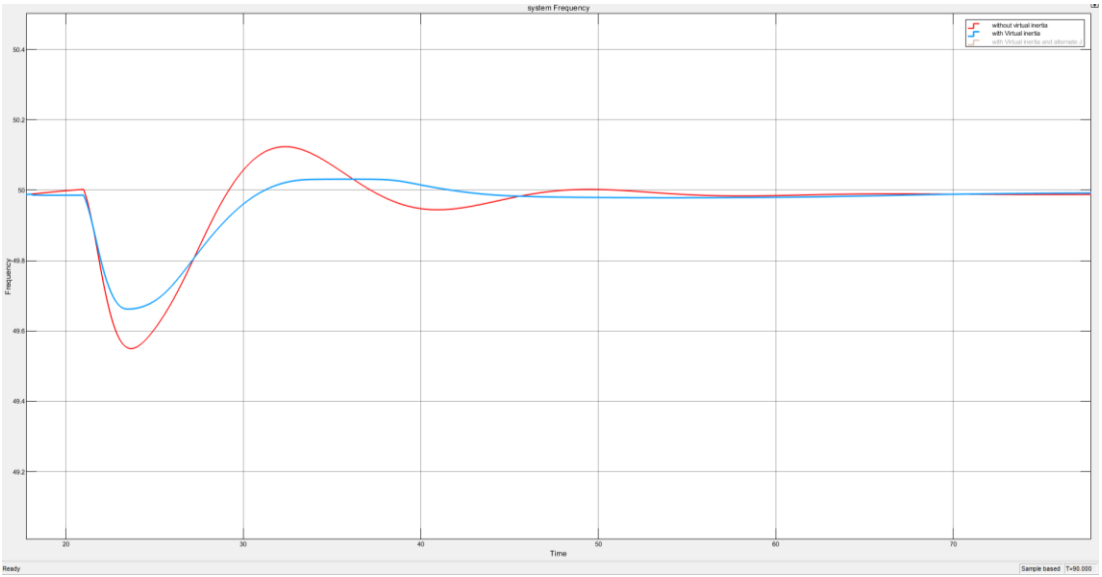

Figure 4.4: Frequency variation with and without virtual inertia for 5% disturbance from 2.5kW nominal load

Table 4.1: Frequency variation comparison with and without virtual inertia for 5% disturbance from 2.5kW nominal load

Parameters	With virtual inertia J	Without virtual inertia J
Lowest point (Hz)	49.63	49.55
Highest point (Hz)	50.04	50.12
Settling time (s)	7.49	13.18
Quantified value (rad)	16.97	20.35

The peak to peak frequency improvement with virtual inertia J = 28.07%

The settling time is defined as the time it takes for the frequency to settle between 49.99Hz and 50.01Hz after a disturbance.

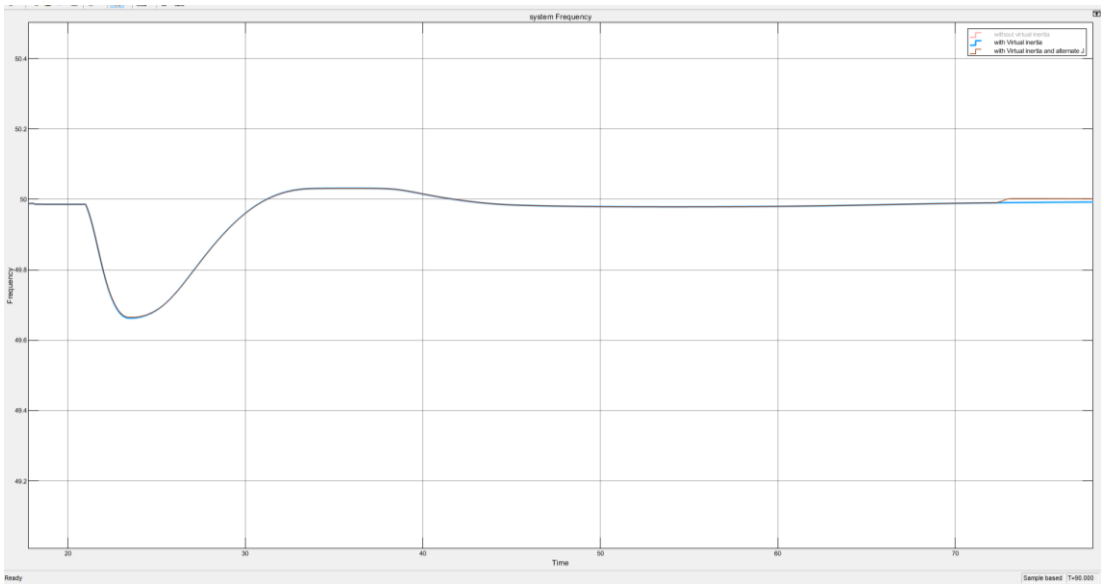

Figure 4.5: Frequency variation with constant and alternating virtual inertia for 5% disturbance from 2.5kW nominal load

Table 4.2: Frequency variation comparison with constant and alternating virtual inertia for 5% disturbance from 2.5kW nominal load

Parameters	With constant virtual inertia J	With alternating virtual inertia J
Lowest point (Hz)	49.63	49.64
Highest point (Hz)	50.04	50.02
Settling time (s)	7.49	7.38
Quantified value (rad)	16.97	14.37

Peak to peak frequency improvement with alternating virtual inertia J = 7.32%

(ii) Results of the system for 10% disturbance from nominal load (5kW)

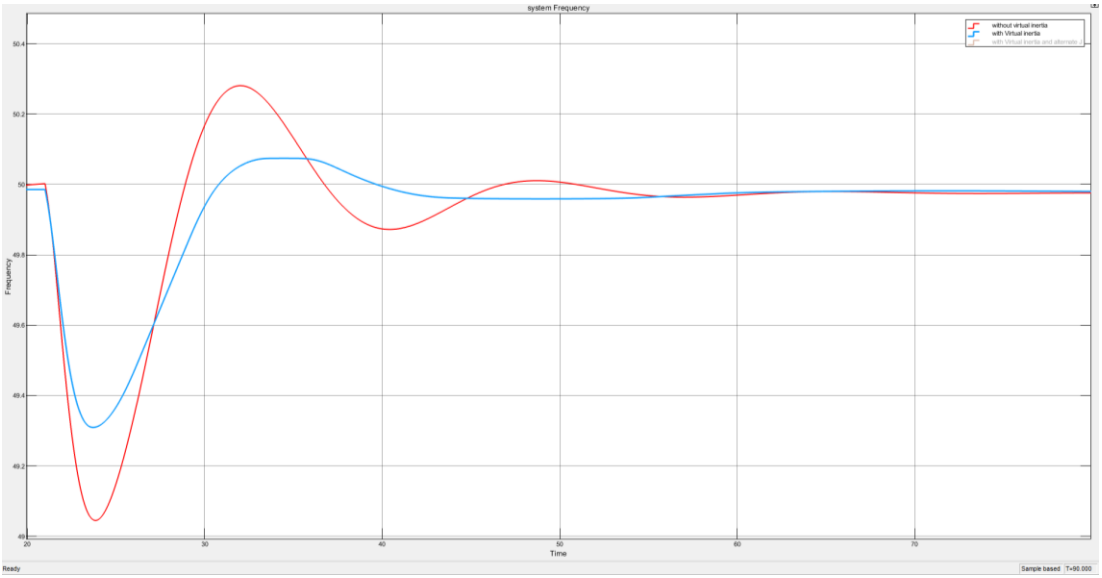

Figure 4.6: Frequency variation with and without virtual inertia for 10% disturbance from 5kW nominal load

Table 4.3: Frequency variation comparison with and without virtual inertia for 10% disturbance from 5kW nominal load

Parameters	With virtual inertia J	Without virtual inertia J
Lowest point (Hz)	49.24	49.05
Highest point (Hz)	50.09	50.28
Settling time (s)	8.22	21.68
Quantified value (rad)	32.57	43.07

Peak to peak frequency improvement with virtual inertia J = 30.89%

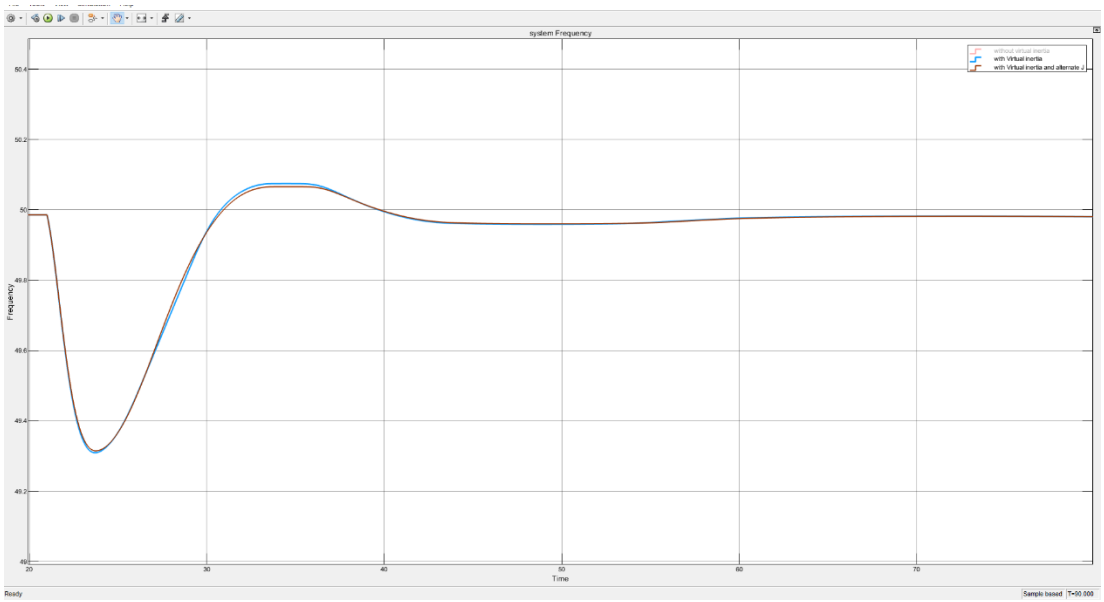

Figure 4.7: Frequency variation with constant and alternating virtual inertia for 10% disturbance from 5kW nominal load

Table 4.4: Frequency variation comparison with constant and alternating virtual inertia for 10% disturbance from 5kW nominal load

Parameters	With constant virtual inertia J	With alternating virtual inertia J
Lowest point (Hz)	49.24	49.25
Highest point (Hz)	50.09	50.07
Settling time (s)	8.22	8.15
Quantified value (rad)	32.57	30.01

Here, the peak to peak frequency improvement with alternating virtual inertia J = 3.53%

(iii) Results of the system for 20% disturbance from nominal load (10kW)

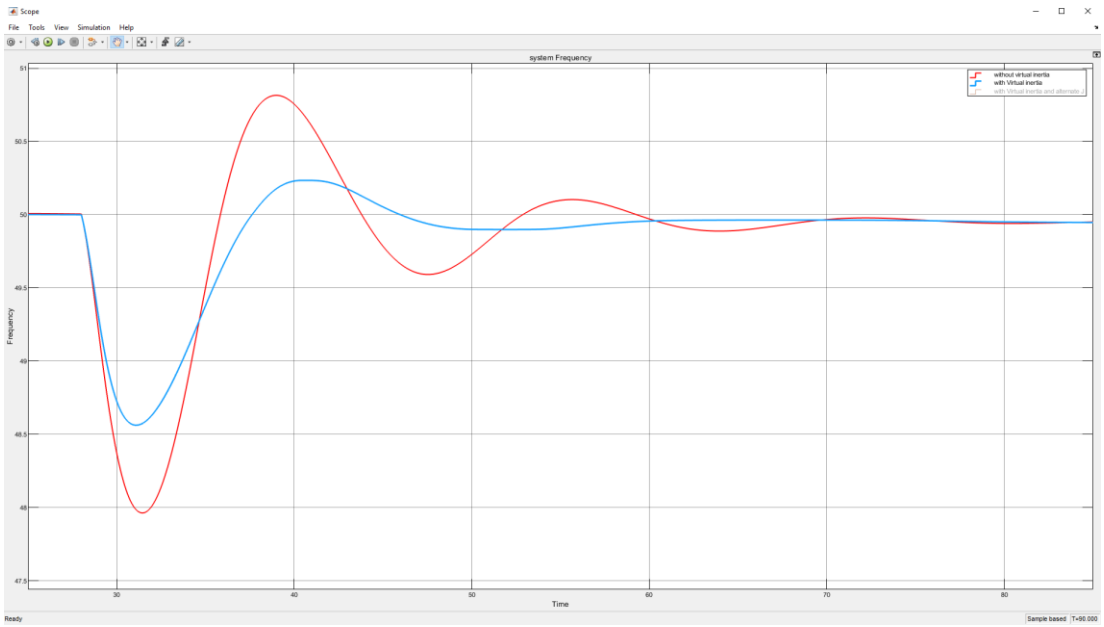

Figure 4.8: Frequency variation with and without virtual inertia for 20% disturbance from 10kW nominal load

Table 4.5: Frequency variation comparison with and without virtual inertia for 20% disturbance from 10kW nominal load

Parameters	With virtual inertia J	Without virtual inertia J
Lowest point (Hz)	48.56	47.96
Highest point (Hz)	50.23	50.81
Settling time (s)	15.97	22.32
Quantified value (rad)	66.7	103.9

Here, the peak to peak frequency improvement with virtual inertia J = 41.4%

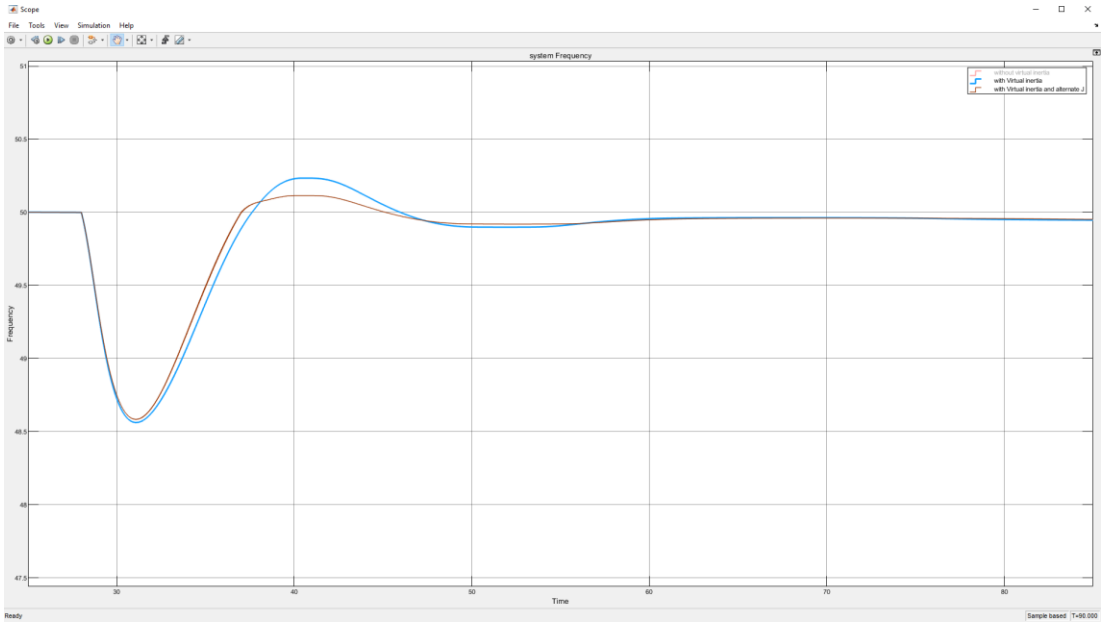

Figure 4.9: Frequency variation with constant and alternating virtual inertia for 20% disturbance from 10kW nominal load

Table 4.6: Frequency variation comparison with constant and alternating virtual inertia for 20% disturbance from 10kW nominal load

Parameters	With constant virtual inertia J	With alternating virtual inertia J
Lowest point (Hz)	48.56	48.58
Highest point (Hz)	50.23	50.11
Settling time (s)	15.97	14
Quantified value (rad)	66.7	61.31

Here, the peak to peak frequency improvement with alternating virtual inertia J = 8.38%. Since peak to peak frequency improvement between constant and alternating virtual inertia is not that much, we can simply use constant virtual inertia J for microgrid systems. Power delivered when constant virtual inertia is incorporated is as follows.

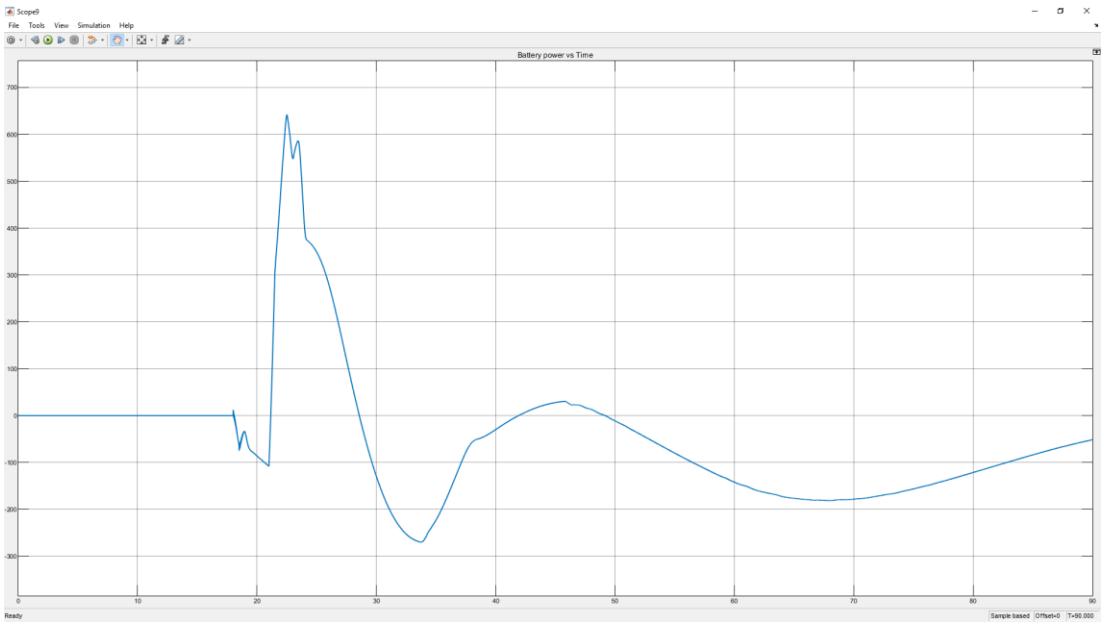

Figure 4.10: Power delivered for 5% disturbance (2.5kW)

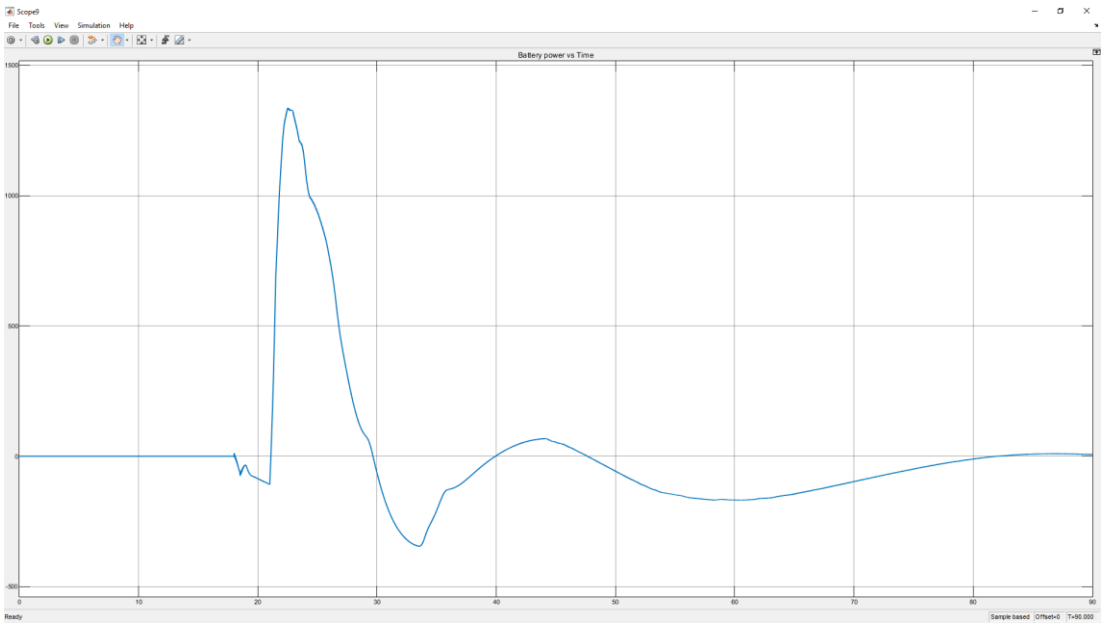

Figure 4.11: Power delivered for 10% disturbance (5kW)

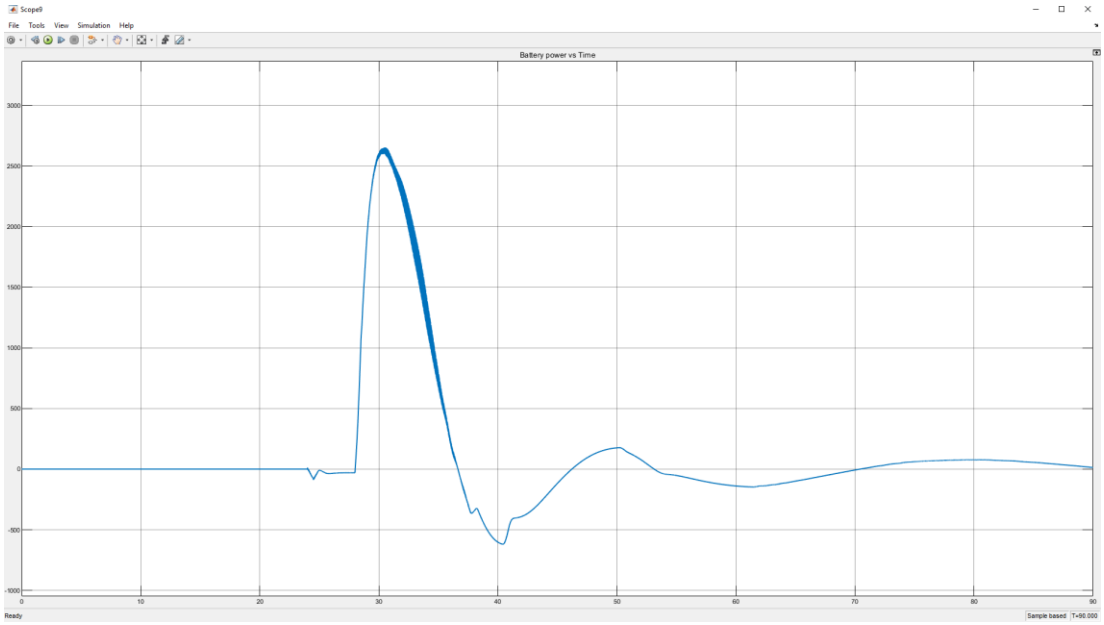

Figure 4.12: Power delivered for 20% disturbance (10kW)

4.3 Results and test conditions for high power system

A load step is applied to the generator to simulate a disturbance and the test parameters are as follows.

Nominal load = 120MW

System voltage = 13.8kV

Inverter/voltage source voltage = 15kV

Nominal frequency = 50Hz

Disturbance = 10MW

Generator Inertia constant = 4s

Rated apparent power = 200MVA

Table 4.7: Frequency variation comparison with and without virtual inertia for high power system

State	Settling Time (s)	High Peak Frequency (Hz)	Low Peak Frequency (Hz)
With Virtual Inertia (Constant J)	23.78	50.23	49.01
Without Virtual Inertia	34.94	50.44	48.77

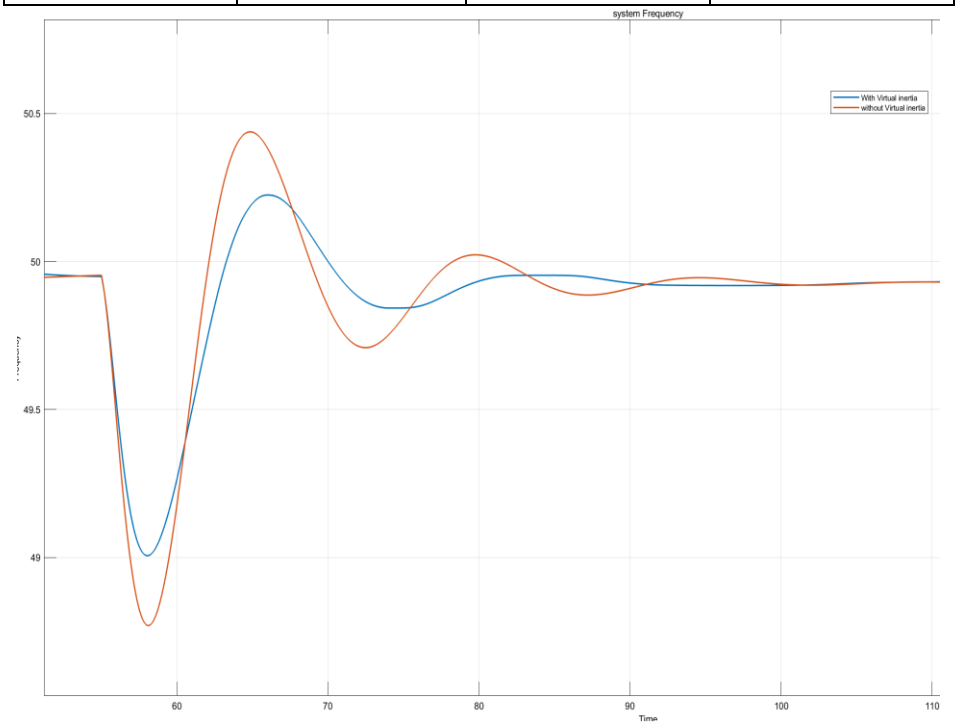

Figure 4.13: System frequency with and without virtual inertia

Figure 4.13 shows the frequency variation of the grid with and without the virtual inertia for a disturbance. As shown in the graph, the system with the virtual inertia shows dramatically better results than the default system without virtual inertia injection. As you can see, the maximum overshoot and the settling time are reduced in this system.

As shown in the Table 4.7, the settling time (Between range 49.99 – 50.01 Hz) is less when virtual inertia takes effect. Here, the settling time with virtual inertia J is 23.78s and the settling time without virtual inertia is J is 34.94s. With virtual inertia, there's a settling time improvement of 31.94%.

Also, high peak frequency with virtual inertia is 50.23Hz and high peak frequency without virtual inertia is 50.44Hz. The low peak frequency with virtual inertia is 49.01Hz and low peak frequency without virtual inertia is 48.77Hz. Therefore, peak to peak frequency with virtual inertia is 1.22Hz and peak to peak frequency without virtual inertia is 1.67Hz. So, the improvement of the peak to peak frequency with virtual inertia is 26.95%.

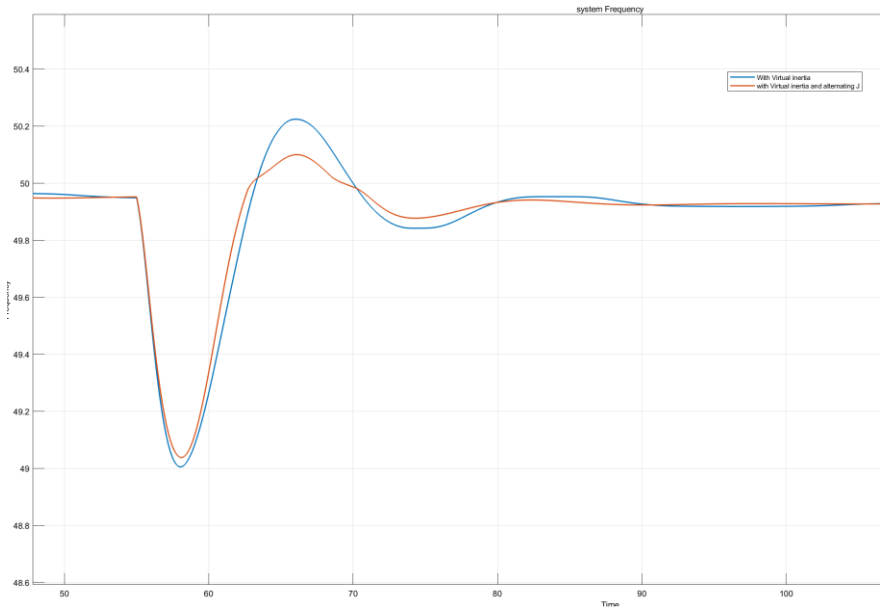

Figure 4.14: System frequency with constant and alternating virtual inertia J

Figure 4.14 shows the frequency change with constant virtual inertia J and with alternating virtual inertia J. The system with the alternating virtual inertia J shows a better improvement than the system with the constant virtual inertia J. Here, the maximum overshoot and the settling time are reduced after alternating virtual inertia J is used.

Table 4.8: Frequency variation comparison with constant and alternating virtual inertia for high power system

State	Settling Time (s)	High Peak Frequency (Hz)	Low Peak Frequency (Hz)
With Constant Virtual Inertia (Constant J)	23.78	50.23	49.01
With Variable Virtual Inertia (Variable J)	20.28	50.09	49.04

As in the Table 4.8, the settling time (Between range 49.99 – 50.01Hz) is less when variable virtual inertia takes effect. The settling time with constant virtual inertia is 23.78s and the settling time with variable virtual inertia is 20.28s. With the constant virtual inertia J, the settling time improvement is 14.72%.

Furthermore, high peak frequency with constant virtual inertia is 50.23Hz and high peak frequency with variable virtual inertia is 50.09Hz. Also, low peak frequency with constant virtual inertia is 49.01Hz and low peak frequency with variable virtual inertia is 49.04Hz. Therefore, peak to peak frequency with constant virtual inertia is 1.22Hz and peak to peak frequency with virtual inertia is 1.05Hz. The improvement of the peak-to-peak frequency with variable virtual inertia is 13.93%.

The frequency deviations can be quantified by a measure introduced as the total oscillation angle. That is the total angle deviation from a rotor at steady state this can be defined by the following equation

$$Angle\ deviation = \int 2\pi |f - f_0|\, dt$$

f - frequency

f_0 – nominal frequency before the disturbance

Measured angle deviation data from the simulation are as follows,

Without Virtual Inertia - 79.23 rad

With constant J - 67.2 rad

With variable J - 59.38 rad

According to above data, total angle deviation from the steady state can be minimized using virtual inertia and with constant J it can be improved 15.18% compared to system without virtual inertia. Also, when the system is without virtual inertia J compared with system with variable virtual inertia J, it is improved by 25.05%.

It is also possible to use the maximum energy of the oscillation as a measure and it can be calculated as follows,

$$Max.energy\ of\ oscillation = \frac{1}{2}J[2\pi(f_L - f_0)]^2$$

f_L – Low peak frequency

f_0 – nominal frequency before the disturbance

J – Inertia constant of the generator

Calculated Maximum energy Oscillation as follows,

Without Virtual Inertia = 484.5kJ

With constant J = 313.6 kJ

With variable J = 294.84kJ

According to above data also it is clear that there is a significant improvement in system when virtual inertia J is injected to the system. It can be further improved using a variable J instead of constant J.

Average power injected to the grid by the virtual inertia system can also be plotted. Here, the system is set to inject no real power during steady state. The plots are as follows,

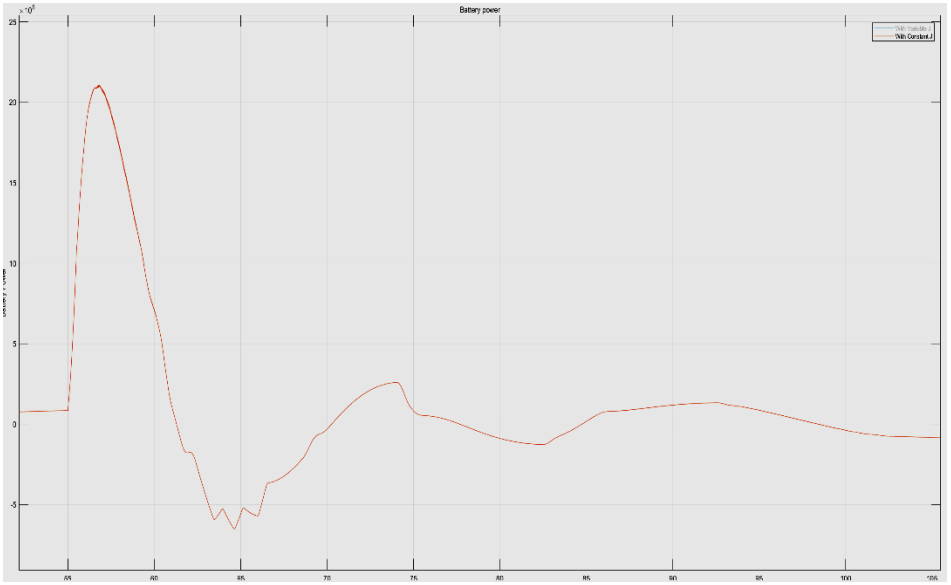

Figure 4.15: Injected power with constant virtual inertia J

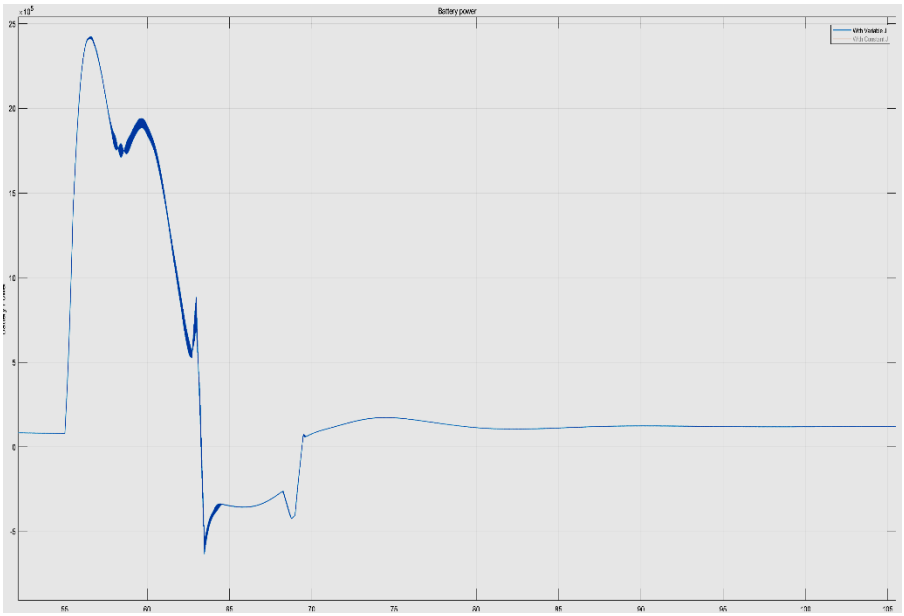

Figure 4.16: Injected power with variable virtual inertia J

The virtual inertia controller adjusts the phase difference between the grid voltage and the inverter voltage. The phase differences between the grid voltage and inverter terminal voltage can be seen in Figure 4.17, Figure 4.18 and Figure 4.19.

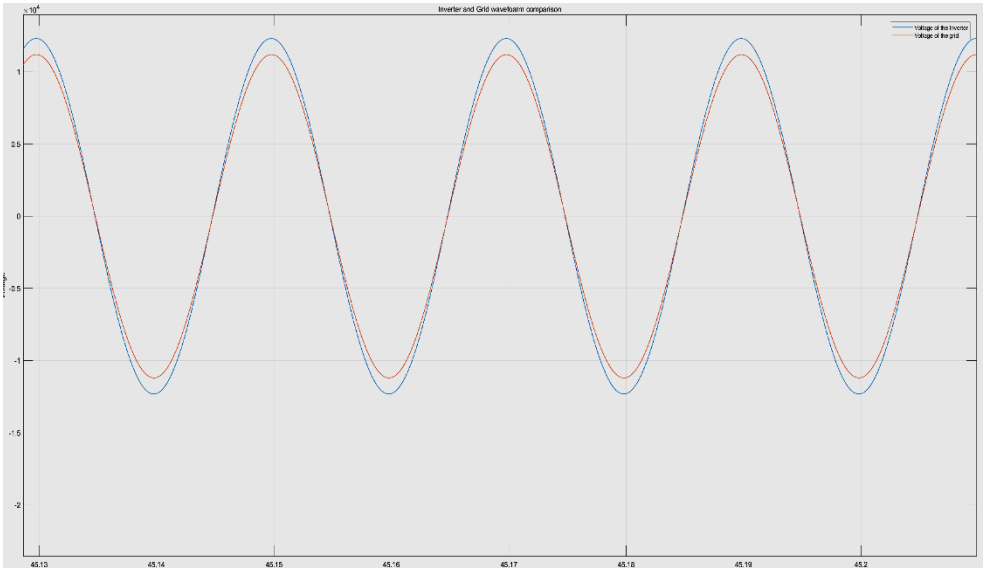

Figure 4.17: Voltage waveform under steady state condition

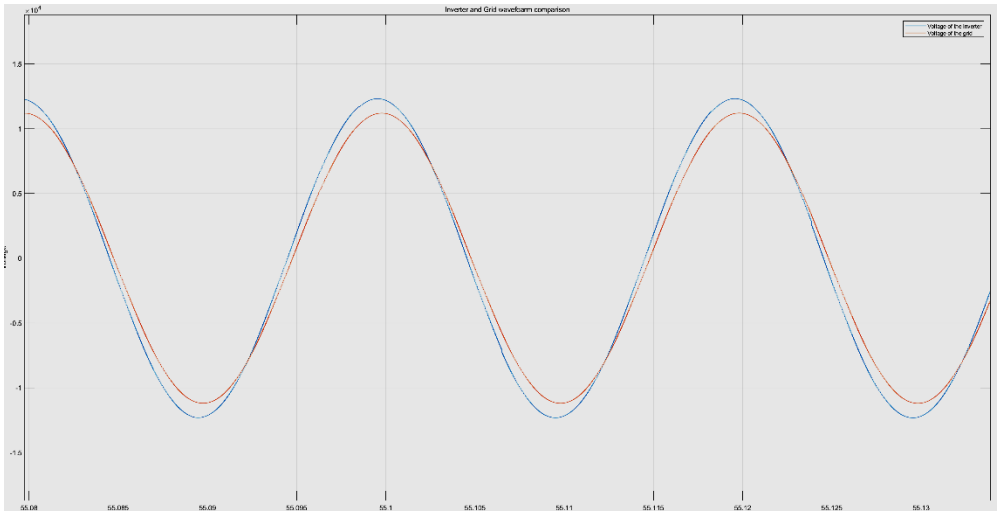

Figure 4.18: Voltage waveform at a disturbance

We can see how the voltage waveform of the virtual inertia system leads the grid voltage to inject power into the grid under a disturbance.

Figure 4.19 depicts the variation of phase angle difference during a disturbance/load step

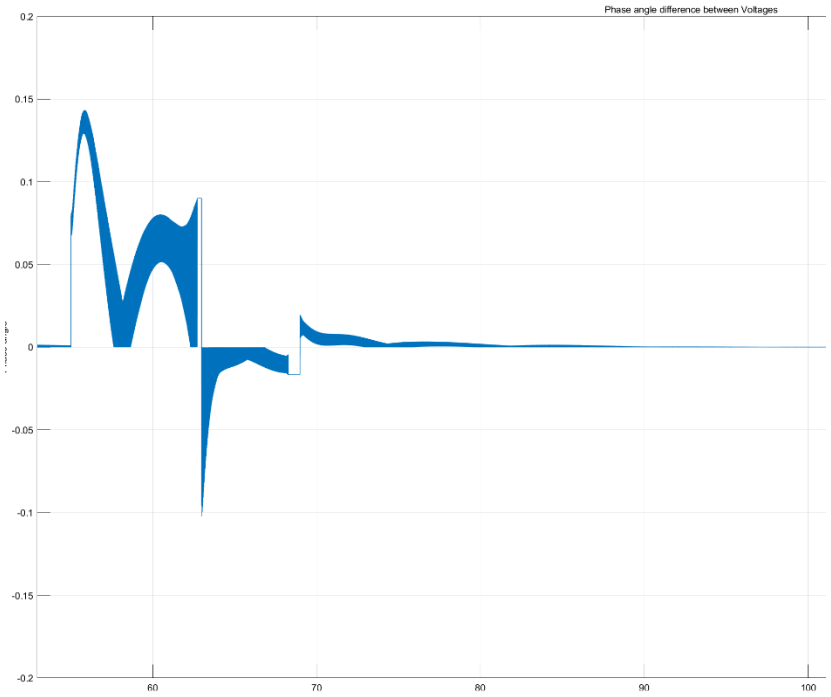

Figure 4.19: Phase angle difference between grid and inverter voltages

4.4 Results and test conditions for multi generator system

Since there is a significant improvement when alternating virtual inertia J is incorporated in high power systems, we can consider alternating virtual inertia J for multi generator system too.

Specifications for the multiple generator system,

Nominal load = 100MW

System voltage = 13.8kV

Inverter/voltage source voltage = 15kV

Nominal frequency = 50Hz

Disturbance = 20MW

Number of generators = 3

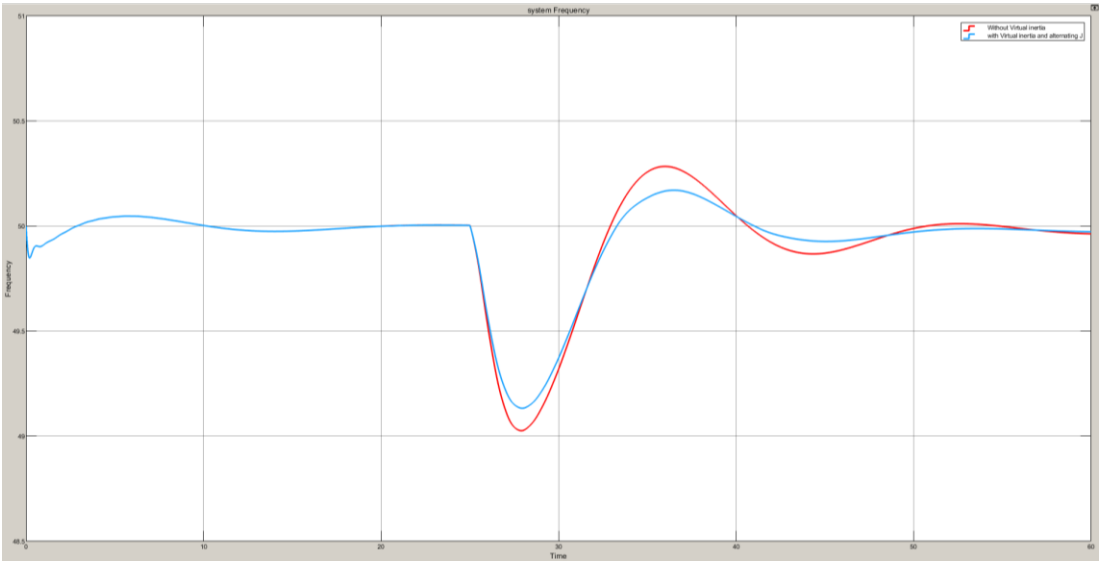

Figure 4.20: Frequency variation with and without virtual inertia J for multi generator system

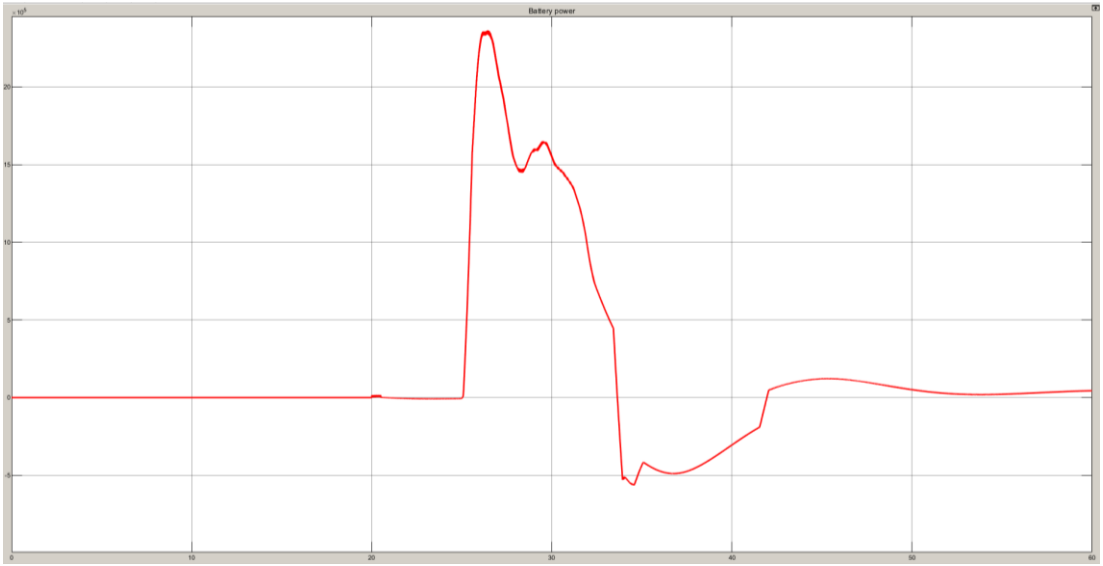

Figure 4.21: Power injected to the multi generator system

4.5 Analysis of the results

Maximum value that can get the system unstable for a 20% disturbance (20% from the nominal Load) was taken by experimental method for a particular nominal Load Value. Then the following graph can be plotted from the obtained data points.

Technically, for a particular load value any J value under the curve is feasible to get results without getting unstable. To apply a safety margin, use 50% of the of the J value that the graph output. So below equation gives optimal J value for this controller in LV system.

$$|J| = 0.5(6E\text{-}07P^2 + 0.0007P + 0.1072)$$

J = Inertia constant

P = Nominal load

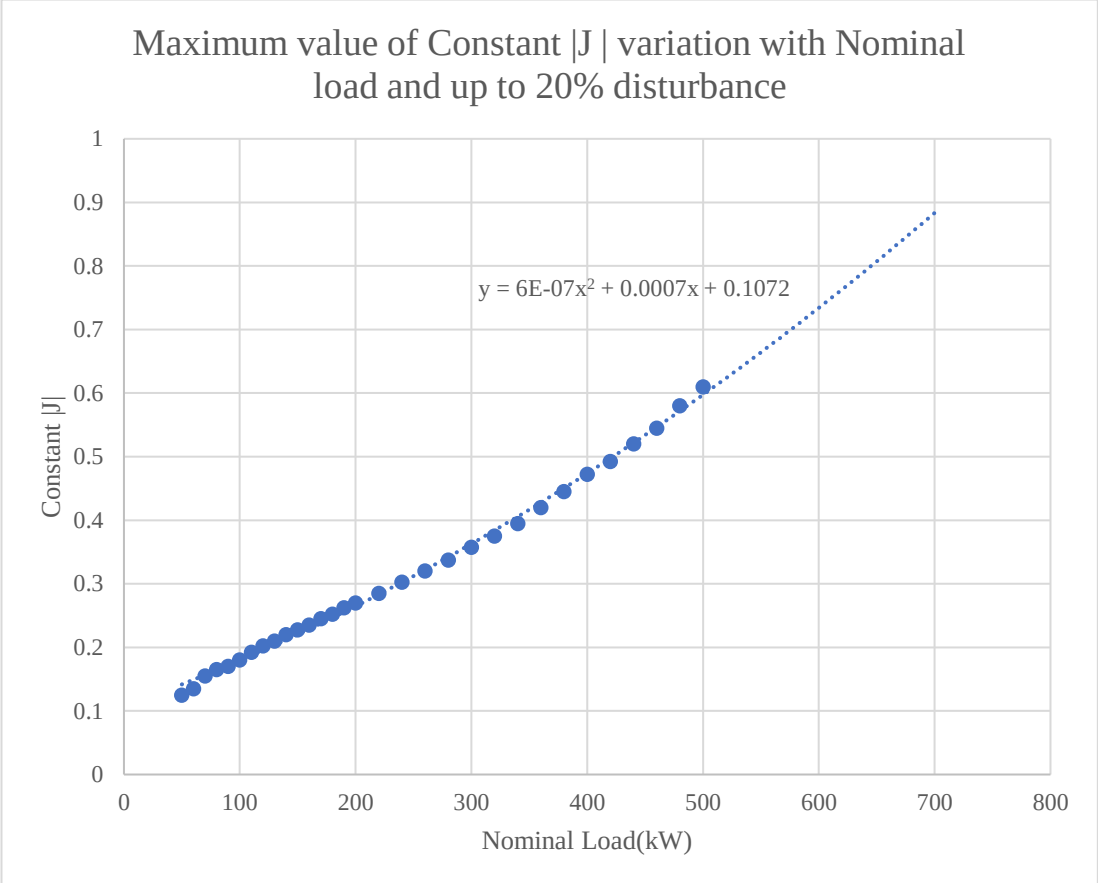

Figure 4.22: Maximum value of constant |J| variation with nominal load and up to 20% disturbance

5. Conclusion

This project report describes a virtual inertia system that injects power into the grid based on the rate of change of frequency and the frequency deviation. And incorporates an alternating inertia strategy. This is less computationally intensive than numerically solving the swing equation as described in the other commonly used method.

From the results we can see the initial frequency drop from the load step, and the subsequent recovery by the governor action and how a virtual inertia system aids in limiting frequency fluctuations and results in an improved response. The performance of a constant inertia virtual inertia system and alternating parameter virtual inertia system was also observed.

In order to test the functionality of the system, different levels of load steps were applied (up to 20% of nominal load) and the frequency plots were obtained. Furthermore, the transfer function obtained for this kind of virtual inertia system allows the system to be incorporated to the frequency control block diagram of a power system for stability analysis.

In conclusion, the simulations conducted on the system demonstrate that a virtual inertia system as described in this report is capable of significantly improve the frequency response of a power system under disturbance due to a load step. The system response to faults were not studies in this paper and would be a topic for future research.

References

[1] J. Alipoor, Y. Miura and T. Ise, "Power System Stabilization Using Virtual Synchronous Generator With Alternating Moment of Inertia," in *IEEE Journal of Emerging and Selected Topics in Power Electronics*, vol. 3, no. 2, pp. 451-458, June 2015, doi: 10.1109/JESTPE.2014.2362530.

[2] M. A. Torres L., L. A. C. Lopes, L. A. Morán T. and J. R. Espinoza C., "Self-Tuning Virtual Synchronous Machine: A Control Strategy for Energy Storage Systems to Support Dynamic Frequency Control," in IEEE Transactions on Energy Conversion, vol. 29, no. 4, pp. 833-840, Dec. 2014, doi: 10.1109/TEC.2014.2362577.

[3] J. Liu, Y. Miura, H. Bevrani and T. Ise, "Enhanced Virtual Synchronous Generator Control for Parallel Inverters in Microgrids," in IEEE Transactions on Smart Grid, vol. 8, no. 5, pp. 2268-2277, Sept. 2017, doi: 10.1109/TSG.2016.2521405.

[4] M.P.N van Wesenbeeck1 , S.W.H. de Haan , Senior member, IEEE, P. Varela and K. Visscher 'Grid Tied Converter with Virtual Kinetic Storage'

[5] M. Surprenant, I. Hiskens and G. Venkataramanan, 'Phase locked loop control of inverters in a microgrid'